Dynamic Stall and Flow Reattachment Studies of a Wind Turbine Blade Section in the Pitching Motion

Mohammad Reza Soltani and Mehdi Seddighi

Department of Aerospace Engineering, Sharif University of Technology, 14556
Azadi Av., Tehran, Iran, mehdisedighi@gmail.com

Abstract. A section of a 660 KW wind turbine blade has been tested in a wind tunnel. Special emphasize was taken on the flow phenomenon near the static stall angle of attack when oscillating the model. In addition to the steady tests, various unsteady tests including the effects of reduced frequency, mean angle of attack, and amplitude have been preformed. Increasing the reduced frequency delays separation infancy, increases lift and degrades the dynamic stability in comparison to the static results. Further it delays the flow reattachment in the downstroke portion of the motion, when the angle of attack decreases. The results show strong effects of initial angle of attack, amplitude of oscillation, and free stream turbulent intensity on the dynamic stall and the flow reattachment processes.

Key words: dynamic stall, flow reattachment, reduced frequency, turbulent intensity.

1. Introduction

Dynamic stall is a very complex phenomenon occurring on helicopter rotor blades, many modern aircraft, blades of turbo machinery as well as wind turbine blades [1-5]. In all cases, dynamic stall is a limiting factor as high speed and maneuver flight capabilities of helicopters as well as limited power production of the wind turbines are concerned [1].
Maximum output power obtained from the wind turbine, usually occurs near the blade stall angle of attack condition. Almost all flying vehicles (except military aircraft) avoid stall as much as possible because of the associated high loads and the possible loss of aerodynamic damping. One of the unsteady, nonlinear aerodynamic problems of significant importance on wind turbines is “dynamic stall" phenomenon [5]. Since many wind turbines rely on stall, especially stall regulated ones, a thorough understanding of the unsteady (deep) stall is necessary [6, 7].

Two advantageous qualities of dynamic stall flow due to development and shedding of the dynamic stall vortex are lift augmentation and stall delay. However, detrimental aspects of dynamic stall arise following the flow separation and shedding of the vortex into the wake that causes not only the lift lost, as in the steady flow stall, but there exists large excursions in the drag and

pitching moment. Moment fluctuations are sever enough to cause structural damage on vehicles experiencing dynamic stall [1]. The development of a dynamic stall flow depends on numerous parameters such as the free stream Mach and Reynolds numbers, the profile of the airfoil, the reduced frequency, the type of oscillation, free stream turbulent intensity, surface contamination, and amplitude of oscillation [2, 8-10].

The dynamic overshoot of $C_{l_{\max}}$ is caused by the two viscous flow effects at moderate amplitudes and frequencies (There is additional effect of the "spilled leading edge vortex" that occurs at large amplitudes and high frequencies). One of the aforementioned phenomenon is due to the integrated effect of the time-lagged external pressure gradient on the boundary layer development and the other one is called "leading edge jet" effect. As the airfoil leading edge moves upward, boundary layer between the stagnation and separation points experiences a moving wall/wall jet effect very similar to that observed on a rotating cylinder. Thus, the boundary layer has a fuller profile than in the steady case and does not separate easily. On the "downstroke" the effect is the opposite, promoting separation [10, 11]. During the phase of dynamic stall onset the concentrated vortex starts to develop and lifts off of the upper surface of the blade rapidly. This procedure is influenced by the different flow phenomena: In a low Reynolds number flow transition from laminar to turbulent plays an important part in the development of the flow close to the airfoil leading edge. One or more separation bubbles may develop and transition takes place over these bubbles [1, 12].

If the boundary layer is too thick, flow separation and dynamic stall onset happen too early. Separated flows are not only common at stall conditions but also it may occur well below stall for laminar flow airfoils operating at a chord Reynolds numbers of approximately nine million or less. These airfoils encounter separation bubbles at the onset of pressure recovery, potentially an important source of unsteady loading and noise. Laminar separation bubbles or transition bubbles are a common phenomenon on airfoils operating at chord Reynolds number less than approximately nine million. Depending on the airfoil shape and on the free stream Reynolds number, these regions of separated flow occur in the leading-edge region and govern the stall characteristics of the single and multi-element airfoils. On laminar flow airfoils, these bubbles also occur at lower angles near the onset of pressure recovery. Bubble-induced vortex shedding phenomenon causes significant oscillations in the airfoil surface pressure signature, hence, affecting aerodynamic forces significantly [13].

An understanding of the reattachment process is essential to alleviate the stall flutter and to improve the dynamic lift characteristics of an oscillating airfoil [14]. To clarify the dynamic stall and flow reattachment behaviour of a section of a 660kw wind turbine blade, series of experimental tests have been conducted. Furthermore, effect of surface contamination and free stream turbulent intensity on the surface pressure signatures, loads and moment coefficients were investigated. Static data for all cases were acquired and are served as the baseline.

2. Experimental Facility

All tests were conducted in the subsonic 0.8m*0.8m*2m closed circuit wind tunnel in Iran. The tunnel operates at speeds from 10 to 100 m/sec. A 25 cm constant chord airfoil model was designed and manufactured for the test program. Figure 1 shows the airfoil section along with the 64 pressure ports located on its upper and lower surfaces used for static and dynamic pressure measurements. The pressure ports are located along the chord at an angle of 20 degrees with respect to the model span to minimize disturbances from the upstream taps. The model was constructed from several layers of composite lay up of altering fiberglass and carbon fiber over ribs. After the production, the model was digitized to ensure the true airfoil coordinate. Due to high number of pressure ports, 64, and size of the selected pressure transducers, it was not possible to place the transducers inside the model. Therefore, extensive experiments were conducted to ensure that the time takes for the pressure to reach the transducers is much less than the frequency response of the transducers themselves, nominally 1msec, and finally the tube length and material that gave minimum time lag for all applied pressures was selected [15]. The angles of attack for the steady case were from -7 to 0 degrees then from 0 to 28 degrees and back to zero. The pitch rotation point was fixed about the wing quarter chord. The oscillating system pitched the model at various amplitudes, means angles of attack, and reduced frequencies. The model angle of attack was varied sinusoidally as $\alpha = \alpha_{\circ} + \overline{\alpha}\sin(2\pi ft)$.

Data were acquired and processed from 64 surface pressure taps, 2 individual tunnel pressure transducers, and an angle of attack encoder using an analog to digital board capable of a sample rate of 500 kHz. Dynamic oscillatory data were then digitalized and digitally filtered using low pass filter with various cut-off and transition frequencies to find the best frequencies to fit the original data, Fig. 2 [16]. All oscillatory data presented here are an average of several cycles and were corrected for the solid tunnel sidewalls and the wake blockage effects [17]. Data were acquired at Reynolds numbers of $0.42\times10^6, 0.63\times10^6, 0.84\times10^6$, 1.12×10^6, and 1.4×10^6. In order to have different inflow turbulent intensities, T.I., a turbulent screen

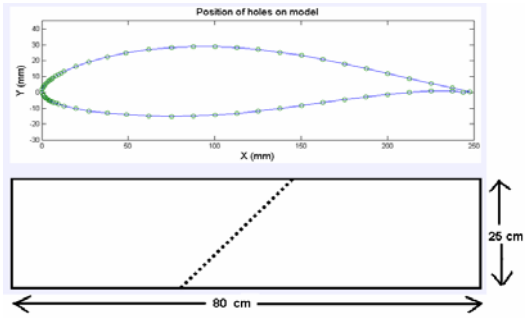

Figure 1. Airfoil section and location of the pressure ports

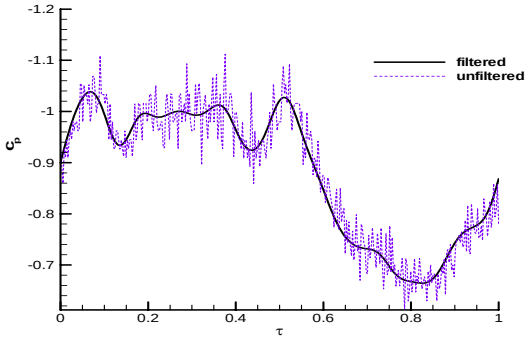

Figure 2. Sample of filtered and unfiltered data.

was added at the beginning of the tunnel test section. In this way, we ensured that the turbulent was homogenous and isotropic in the entire test section. Because of the existence of screen, for the higher T.I. case, the tests were conducted at the Reynolds numbers of 0.42, 0.63, and 0.84 million only. The measured values of the turbulence intensities inside the test section are presented in Fig. 3.

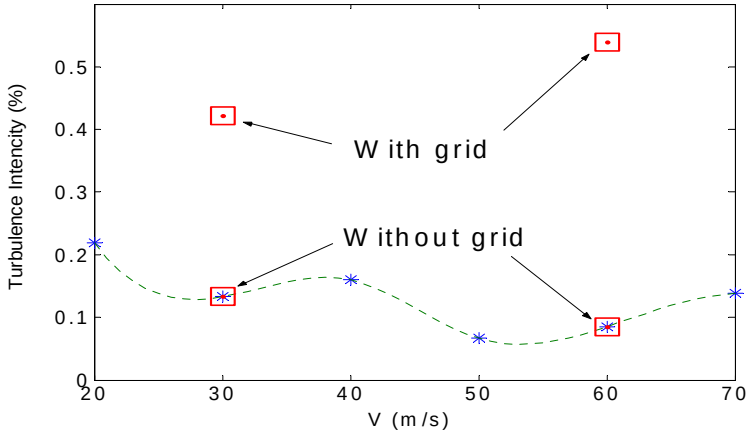

Figure 3. Wind tunnel turbulent levels.

3. Results And Discussion

As mentioned before, the main purpose of this study is to examine the effects of unsteady parameters on the dynamic stall and flow reattachment behavior of a section of a 660KW wind turbine blade. Both dynamic and static data were collected at Reynolds number of $0.42\times10^6 < \mathrm{Re} < 1.4\times10^6$. Dynamic data were obtained at reduced frequencies ranging from 0.005 to 0.11.

Figure 4 depicts variations of the unsteady pressure coefficients on the airfoil at three angles of attack, 7, 11, and 14 degrees, during both upstroke and downstroke motions when the model is oscillating in such a way that its motion covers below and beyond the static stall angle of attack, $\alpha_{\max,dyn.} < \alpha_{stall,static}$ and $\alpha_{\max,dyn.} > \alpha_{stall,static}$.

It is seen that in the upstroke motion at an angle of attack of 7 degrees, Fig. 4a, the main effect of the reduced frequency is exposed in the region of the model surface, $x/c \le 0.4$. Thus, the static pressure coefficient of $\left|C_{p_.}\right|_{static} = 1.8$ reduces to $\left|C_{p_{\min.}}\right|_{dynamic} = 1.38$ for k=0.06. This reduction is emanated from the unsteady wake shedding and the induced curvature effects that occur during the dynamic motion of the model when its angle of attack is below the static stall A.O.A[1] and in the upstroke motion. As a result, the normal force coefficient for the dynamic case is less than its corresponding static value. When the model continues its upstroke motion and its dynamic A.O.A reaches the static stall one, $\alpha \cong 11^\circ$, the delay in the separated flow region caused by the dynamic motion

[1] angle of attack

varies the c_p distribution as seen from Fig. 4a. This phenomenon will result in an increase of lift in comparison to its corresponding static value. Therefore, dynamic normal force is less than the static value for the dynamic angle of attack less than the static stall angles while in the post stall region dynamic data overshoot their corresponding static values.

In the downstroke portion of the motion, Fig. 4b, at $\alpha = 14^\circ$ the separated flow does not reattach until the A.O.A. is reduced to about $\alpha \cong 11^\circ$, when the reattachment process start and the effect of k in this case is noticeable.

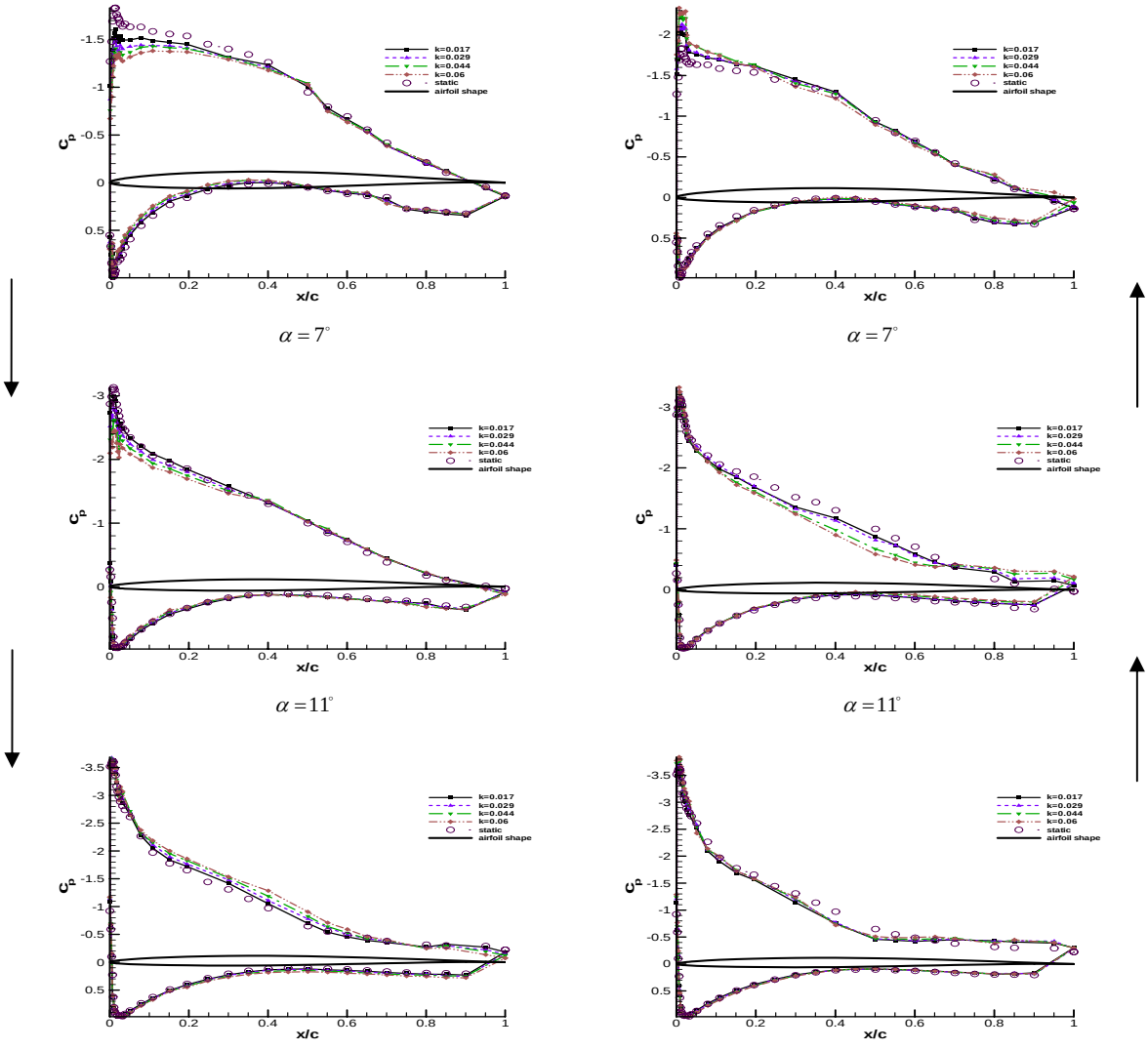

Figure 4. Effect of reduced frequency on the unsteady pressure distribution, $\alpha = 10 + 5\sin(\omega t)$, $\mathrm{Re} = 0.64 \times 10^6$.

From Fig. 4b, it is seen that the flow reattaches the entire upper surface when the A.O.A. is reduced about 7 degrees. Furthermore, as k increases, the aforementioned angle decreases.

Figure 5 shows the effect of reduced frequency on the entire 64 pressure ports for both upstroke and downstroke motions. In addition, the results are for the cases when the model is oscillated around the static stall angle of attack, $\alpha = 10 + 5\sin(\omega t)$, and also for oscillation beyond the $\alpha_{stall,static}$ completely, $\alpha = 18 + 5\sin(\omega t)$. Although, the effect of increasing reduced frequency from k=0.017 to k=0.06, is not significant, it influences the separated flow on the upper surface, Fig. 5a. Furthermore, the improvement is seen to be more affected for pressure ports located near the leading edge, $x/c \le 0.5$. Thus, for the next figure, the pressure ports located in this region is investigated in more detail.

Figure 6 depicts the effect of increasing k on the pressure signatures of various pressure ports during the entire oscillation cycle. For the pressure port close to the L.E., $x/c \le 0.07$, the pressure history trend for all k is similar to the sinusoidal motion of the model which indicates that the flow remains attached to the surface. On the other hand, a time lag is seen when the reduced frequency is varied. For pressure ports located at $x/c \le 0.05$, Fig. 6 shows similar phenomenon where increasing k leads to an increase of the suction peak value. However, for the pressure ports located at $x/c > 0.05$, the variation of c_p with τ differs from those at $x/c \le 0.05$, Fig. 6.

The effect of some important unsteady parameters, k, $\bar{\alpha}$, $\alpha_\circ$, T.I., on the unsteady normal force and pitching moment of the model, is depicted in Fig. 7. Effects of some of these parameters were investigated in more detail and are discussed in Ref. 3. It is seen by inspection that the effect of increasing amplitude on the normal force and moment coefficients, is similar to the reduced frequency increment effect shown previously. Figure 7c shows the effect of small amplitude oscillations, that appear in the wind turbine blades, at a constant amplitude, $\bar{\alpha} = 2^\circ$, on c_n and c_m coefficients. It is seen that the width of the hysteresis loop is decreased with increasing the initial angle of attack up to $\alpha_\circ = 10^\circ$. Furthermore, at this A.O.A., $\alpha_\circ = 10^\circ$, the cross over is seen at the curve which indicates the occurrence of separation followed by the reattachment process at an A.O.A. of about $\alpha \approx 8.5^\circ$. At the same time, the width of the hysteresis loop for the pitching moment coefficient curve decreases which shows reduction of the dynamic stability during dynamic stall occurrence. On the other hand, at high alpha oscillations when the model is near $\alpha_{static,stall}$ in the upstroke motion, the hysteresis loop is widened and its direction is clockwise. Note, for the low alpha oscillation case as seen from Fig. 7c, the direction of the cn curve is contraclockwise. With going far beyond the static stall angle of attack, the width of the hysteresis loop increases more, Fig. 7c.

One of the most interesting parameter which affects the dynamic stall and flow reattachment phenomena is turbulent intensity of the free stream. This effect on the coefficients of C_n and C_m curves is shown in Fig. 7d. From this figure, it is seen that T.I. has strong influence in the post stall characteristics of both c_n and

c_m curves. However, its influence in the low alpha portion of the curve is minimal, Fig. 7d.

4. Conclusion

Various tests were conducted in the wind tunnel to examine the dynamic stall behaviour and flow reattachment process of a section of a wind turbine blade. Tests were carried out with altering some important unsteady parameters affecting the wind turbine performance such as reduced frequency,

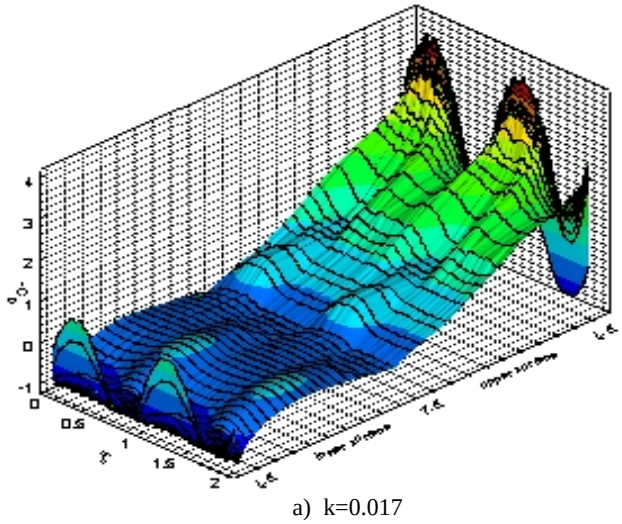

a) k=0.017

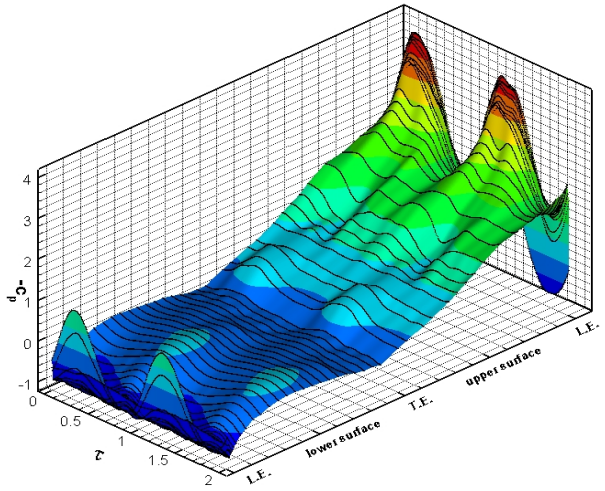

b) k=0.06

a) $\alpha = 10 + 5\sin(\omega t)$

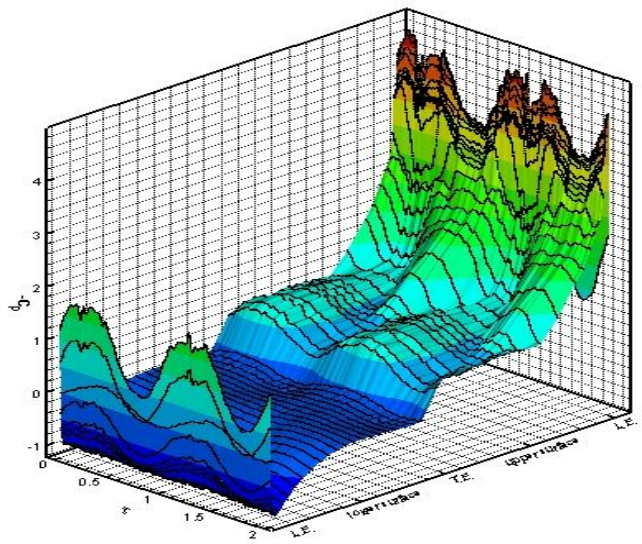

a) k=0.017

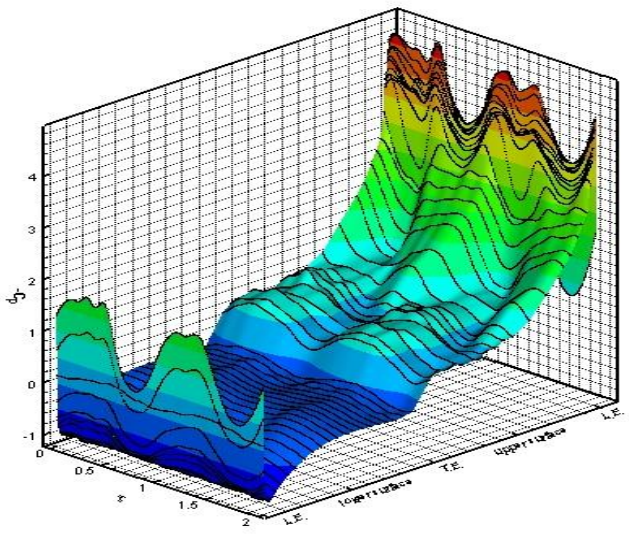

c) k=0.06

b) $\alpha = 18 + 5\sin(\omega t)$

Figure 5. Unsteady surface pressure distribution, $\mathrm{Re} = 0.64 \times 10^6$.

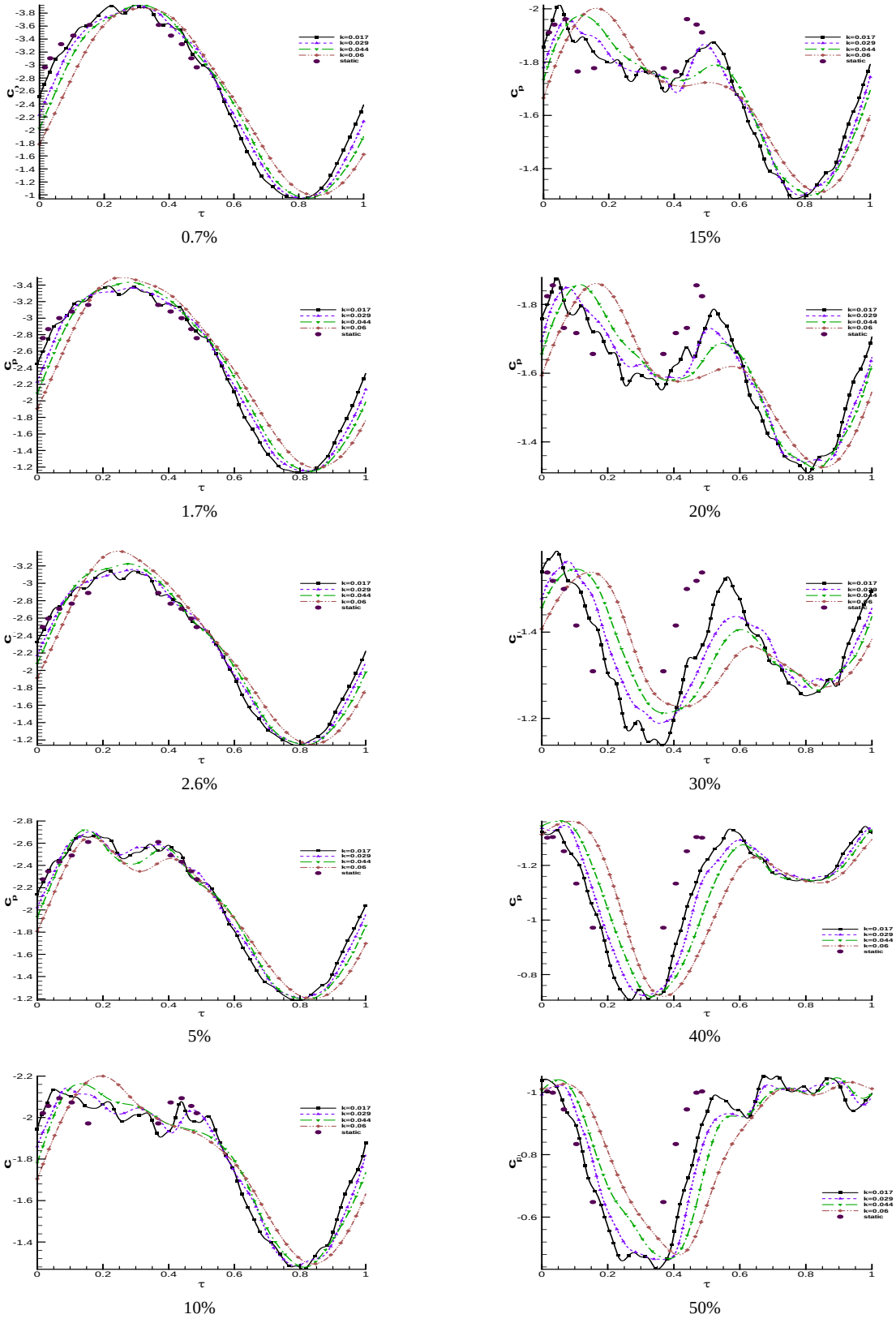

Figure 6. Time history of some upper surface pressure ports, $\alpha = 10 + 5\sin(\omega t)$, $\mathrm{Re} = 0.64 \times 10^6$.

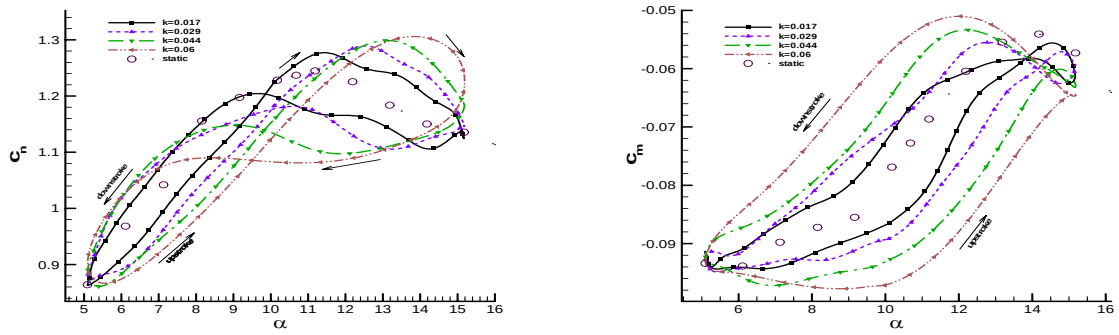

a) Effect of reduced frequency, $\alpha = 10 + 5\sin(\omega t)$.

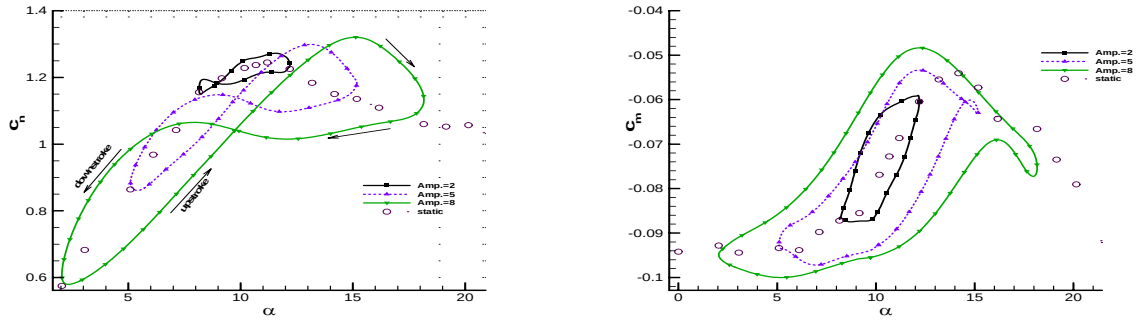

b) Effect of amplitude $\alpha_{\circ} = 10^{\circ}$, $k = 0.044$.

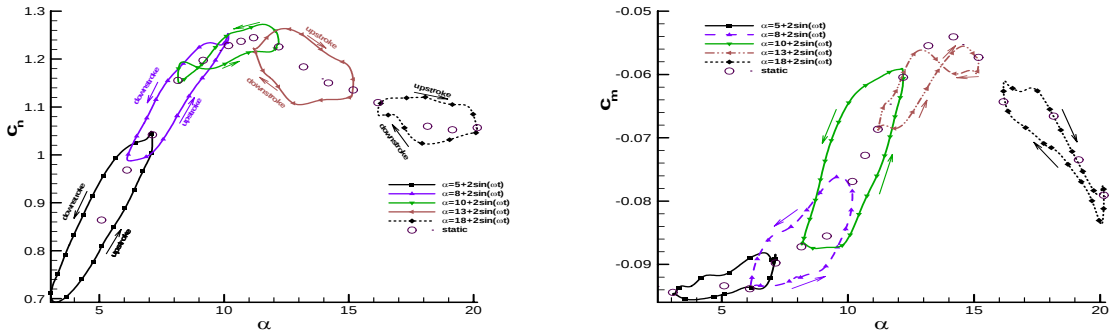

c) Effect of initial angle of attack, $\overline{\alpha} = 2$, $k = 0.044$

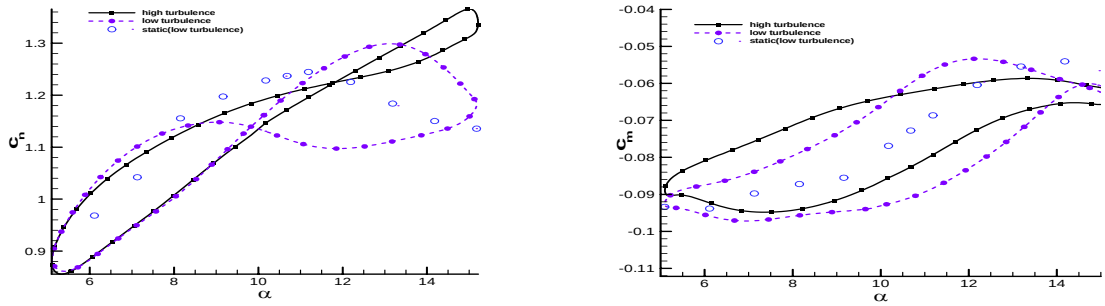

d) Effect of turbulent intensity $k = 0.044$, $\alpha = 10 + 5\sin(\omega t)$.

Figure 7. Effect of various parameters on the c_n and c_m curves, $\alpha = 10 + 5\sin(\omega t)$, $\mathrm{Re} = 0.64 \times 10^6$.

amplitude, initial angle of oscillation, and turbulent intensity of the free stream. Results showed that reduced frequency had strong effect in the infancy and development of the flow separation and finally dynamic stall behaviour of the section under study. Furthermore, increasing the amplitude and initial angle of attack increased the unsteadiness and therefore, led to delaying the reattachment process during the downstroke portion of the oscillatory motion. Conversely, turbulent intensity improved the dynamic stall strongly, and affected the reattachment process swiftly.

Acknowledgment

This work was supported by the Iranian Renewable Energy Organization. Authors would like to thank their cooperation. Furthermore, the collaborative efforts of F. Askari and A. Alizadeh are appreciated.

References

1) Geissler, W., Haselmeyer, H., "Investigation of dynamic stall onset", Journal of Aerospace Science and Technology, May 2006.
2) Wilder, M. C., "Control of Unsteady Separated Flow Associated With the Dynamic Stall of Airfoil", Report of MCAT Institute, 1995.
3) Soltani, M. R., Bakhshalipour, A., Seddighi, M., "Effect of Amplitude and Mean Angle of Attack on the Unsteady Surface Pressure of a Pitching Airfoil", Journal of Aerospace Science and Technology, Vol. 2, No. 4, December 2005, pp. 9-26.
4) Leishman, J. G., "Challenges in modeling the unsteady aerodynamics of wind turbines", AIAA 2002-0037, 2002.
5) Hansen, A. C, Butterfield, C. P, "Aerodynamics of Horizontal -Axis Wind Turbines", Annul Rev. Fluid Mech., 1993.
6) Vermeer, K. J., Sqrensen, J. N., and Crespo, A., "Wind Turbine Wake Aerodynamics", Progress in Aerospace Sciences, Elsevier, 2003.
7) Fuglsang, P., Antoniou, I., Sørensen, N. N., and Madsen, H. A., "Validation of a Wind Tunnel Testing Facility for Blade Surface Pressure Measurements", Risø-R-981(EN), 1998.
8) Mccroskey, W. J., "Unsteady Airfoils", Ann. Rev. Fluid Mech. U.S. Army Aerodynamics Laboratory and NASA, 1982, pp. 285-309.
9) Seddighi, M., Soltani, M., "Effect of Surface Roughness on an Airfoil in Pitching Motion", AIAA, 2006-3918, 36th Fluid Dynamics Conference and Exhibit, Jun 2006.
10) Ericsson, L. E., Reding, J. P., "Unsteady flow concepts for Dynamic Stall Analysis", Journal of Aircraft, Vol. 21, No. 8, Aug. 1984, pp. 601-606.
11) Gerontakos, P. and Lee, T., "An Experimental Analysis of the Flow Over an Oscillating Airfoil".

12) Geissler, W., Trenker, M., "Numerical investigation of dynamic stall control by a nose-drooping device", in: AHS-Aerodynamics, Acoustics and Test Evaluation Technical Specialist Meeting, San Francisco, CA, January 23– 25, 2002.
13) Mayda, E. A., Van Dam, C. P., "Bubble-Induced Unsteadiness on a Wind Turbine Airfoil", Journal of Solar Energy Engineering, Vol. 124, 2002, pp.335-344.
14) Ahmed, S., Chandrasekhara, M. S., "Reattachment Studies of an Oscillating Airfoil Dynamic Stall Flow field", AIAA JOURNAL, Vol. 32, No. 5, 1994.
15) Soltani, M. R., Rasi, F., Seddighi, M., and Bakhshalipour, A., "An Experimental Investigation of Time lag in Pressure Measuring System", AIAC-2005-028, Presented at the 2nd Ankara International Aerospace Conference, Turkey, 2005.
16) Horowitz, P. and Hill, W., *"The Art of Electronics"*, 2nd Edition, Cambridge University Press, UK, 1989.
17) Barlow, J. B., Rae, W. H., Pope, A., *"Low-Speed Wind Tunnel Testing"*, John Wiley & Sons Inc., 3rd edition, 1999.